

Effects of anion concentration on ion-transport pressure in nanopores

Taewan Kim,¹ Weiyi Lu,² Aijie Han,³ Venkata K. Punyamurtula,² Xi Chen,⁴ and Yu Qiao^{1,2,a)}

¹*Program of Materials Science and Engineering, University of California-San Diego, La Jolla, California 92093, USA*

²*Department of Structural Engineering, University of California-San Diego, La Jolla, California 92093, USA*

³*Department of Chemistry, University of Texas-Pan America, Edinburg, Texas 78539, USA*

⁴*Department of Civil Engineering and Engineering Mechanics, Columbia University, New York, New York 10027, USA*

(Received 3 September 2008; accepted 21 October 2008; published online 7 January 2009)

In an experiment on pressure-driven ion transport in nanopores of a zeolite, the anion concentration is varied in a broad range. As the anion concentration is relatively low, its influence on the ion transport pressure, which reflects the system free energy variation rate, is negligible. When the anion concentration is relatively high, it has a pronounced effect on the ion transport pressure, which should be attributed to the unique surface ion structure in the confining nanoenvironment. The testing data also indicate that the effective interfacial tension is highly dependent on the anion size. © 2009 American Institute of Physics. [DOI: 10.1063/1.3023071]

Understanding ion transport in nanometer-sized channels, tubes, and pores is of immense importance to the studies on drug delivery, biomedicine, energy conversion, sensing, catalysis, and many others.^{1–5} As an electrolyte dissolves in a bulk water phase, cations and anions are separated by water molecules. Each solvated ion is usually surrounded by a number of water molecules.⁶ The coordinate number is dependent on the ion size, ion charge, molar concentration, temperature, etc. At a solid surface, the solvated structure is influenced by the solid atoms since the force field across the interface is usually asymmetric.⁷ As the electrolyte solution flows in a large channel, except for the thin interface layer, the ion behavior is quite homogeneous, which can be well described by the classic fluid mechanics.⁸ At the solid-liquid interface, the ions in the inner layer (the Gouy–Chapman layer) are relatively immobile, and the ions in the outer layer (the Stern layer) are relatively mobile.⁹ The net ion motion along the axial direction can lead to a stream current effect,¹⁰ which has been detected in nanochannels as small as 10–50 nm.^{11,12}

As the channel size is smaller than a few nanometers, the continuum theory breaks down, not only because the surface to volume ratio is ultrahigh, but also because the molecular and ion configurations can be directly confined by the nanochannel wall.¹³ Since in such a small channel most of the solvated ions are exposed to the solid phase, the interface zone dominates the liquid properties. Moreover, the mass and energy exchange between the interface layer and the bulk phase is determined by the adsorption, desorption, and diffusion of ions and solvent molecules along the solid surface, as the interior of the nanochannel can no longer serve as an ion reservoir. As a result, the time constant of surface charging and discharging process can be quite large.^{14–16}

The interaction among the solvent/solute molecules and ions with the nanochannel wall has a number of unique characteristics. Even when the nanochannel surface is nominally wettable, the nanochannel size must be much larger than

the molecular/ion size, otherwise the infiltration can be difficult.^{17,18} As an ion is solvated, the size of the water molecule cluster surrounding it is typically in the range of a few to 10 Å. When an ion is in a nanochannel that is of the effective diameter comparable with or smaller than this characteristic length, the solvated structure is distorted.¹⁹ Configurations that would be energetically unfavorable in a bulk phase can be dominant, which significantly affects the system free energy.²⁰ Under this condition, the space may be insufficient for the layered structure that usually exists at a large surface,²¹ which further changes the ion transport behaviors.

One of the fundamental questions that still remain unanswered is, in a nanochannel, what is the role of anions. At a large solid surface, the anion density in the Gouy–Chapman and the Stern layers tends to be low.²² Therefore, the anion effect on the solid-liquid interfacial properties, such as the interfacial tension, is secondary. In a nanochannel, since anions can directly contact the solid atoms, a squeezing effect can be induced.²³ While a number of computer simulations have been conducted on ion transport behaviors,²⁴ experimental data are still scarce. Furthermore, previous studies in this field were focused on the spontaneous ion adsorption and diffusion procedures. While a few research works^{25,26} were performed on pressurized ion behaviors, the effects of cations and anions were seldom analyzed separately.

In the current study, a Zeolyst ZSM-5 zeolite was investigated. The as-received material was in powder form. The particle size was 10–50 μm. By using a Micromeritics ASAP-2000 analyzer, the nanopore size was measured as 0.6 nm, and the specific surface area was 930 m²/g. It was an aluminosilicate with regular interconnected nanopores. In order to modify its acidity, about 2 g of ZSM-5 zeolite sample was first dried in vacuum at 120 °C for 6 h, and then immediately placed in a vertical reactor, across which a silicon tetrachloride vapor flow was maintained at 400 °C for 2.5 h. After furnace cooling and repeated rinsing in acetone and warm water, the material was transferred to a quartz tube furnace and exposed to an air flow with saturated water steam at 140 °C for 8 h. The steam flow rate was maintained

^{a)}Author to whom correspondence should be addressed. Electronic mail: yqiao@ucsd.edu.

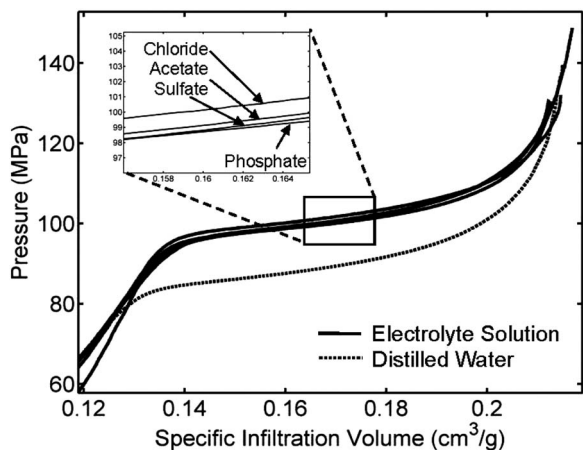


FIG. 1. Typical sorption isotherm curves when the cation concentration is 0.5M. The curves have been shifted along the horizontal direction.

at 25 ml/min. After air cooling, the material was calcined in air at 550 °C for 2 h.

The testing cell was produced by sealing 300 mg of the treated ZSM-5 zeolite sample and 3.5 g of electrolyte solution in a hardened steel cylinder. The electrolyte was sodium chloride, sodium acetate, sodium sulfate, or sodium phosphate. The sodium ion concentration C_0 was either 0.5M or 2M. The sizes of acetate, sulfate, and phosphate anions were somewhat similar. Their ionic charge numbers were 1, 2, and 3, respectively. The liquid phase was compressed by a type-5580 Instron machine through a hardened steel piston, which was sealed by a reinforced O-ring. The cross-sectional area of the piston was 286 mm². When the piston load was sufficiently high, as will be discussed shortly, the pressure induced infiltration would take place and the infiltration plateau in sorption isotherm curve was measured. The piston was stopped once the infiltration was completed. The piston speed was kept at 1 mm/min. Reference experiments were performed by using distilled water as the liquid phase. Typical sorption isotherm curves are shown in Figs. 1 and 2.

The dashed line in Fig. 1 shows the transport behavior of pressurized water molecules. Because the treated ZSM-5 sample is highly hydrophobic, the nanopores remain empty when the zeolite crystals are immersed in water. As an external pressure P is applied on the liquid phase, the average molecular distance in the liquid phase is reduced, and thus the system free energy E increases. The increase in E is

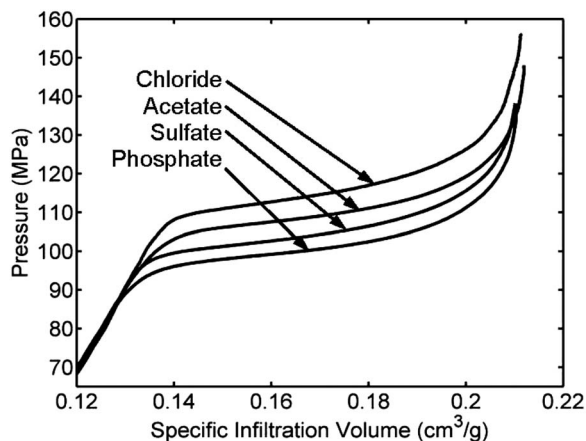


FIG. 2. Typical sorption isotherm curves when the cation concentration is 2M. The curves have been shifted along the horizontal direction.

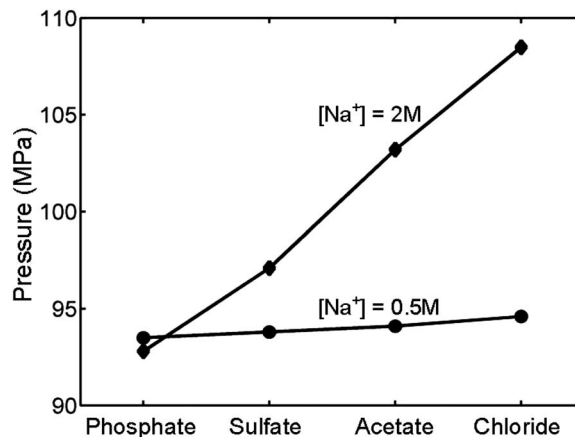


FIG. 3. The ion transport pressures of various electrolyte solutions.

balanced by the mechanical work done by the piston. If the value of P is sufficiently high, the repelling effect of nanopore wall can be overcome, and water molecules start to enter the nanopores. On the one hand, because the zeolite crystals are much stiffer than the liquid phase, the nanopore wall can be regarded as rigid. Under this condition, the influence of the external pressure field inside the nanopores is negligible. Thus, when the liquid phase is confined, the work done by P is released, which can be assessed as $NP(\pi r^2 d)$, where r is the effective nanopore radius, d is the infiltration depth, and N is the number of nanopores. On the other hand, as the hydrophobic nanopore surface is exposed to the liquid phase, the system free energy increases by $N\gamma(2\pi r)d$, where γ is the effective solid-liquid interfacial tension. At the equilibrium condition, $P_i = 2\gamma/r$, with P_i indicating the critical pressure at which the ion transport starts. When P reaches P_i , water molecules keep infiltrating into the nanoporous space with a relatively small pressure increment, and hence an infiltration plateau is formed in the sorption isotherm curve. The infiltration plateau ends when the nanopores are filled. The pressure increase during the infiltration process is probably associated with the column resistance that water molecules must overcome to slide against the nanopore surface.²⁷ From Fig. 2, it can be seen that for the reference system, P_i is about 81 MPa. The effective interfacial tension is $\gamma = P_i r / 2 = 12 \text{ mJ/m}^2$, where r is taken as 3 Å.

With the addition of electrolyte, the main characteristics of sorption isotherm curves are similar. The critical pressure P_i , however, becomes much higher. When the sodium cation concentration C_0 is 0.5M, as shown in Fig. 1, P_i is around 94 MPa. Correspondingly, the effective interfacial tension γ increases to 14.2 mJ/m², higher than that of pure water by nearly 18%. Clearly, with the solvated ions, the repelling effect of nanopore walls is more pronounced, which fits with the prediction of classic theory that the surface tension of an electrolyte solution is higher than that of water. The rearrangement of ion configuration near the solid surface demands additional external work. Thus, with the electrolyte, the system free energy rises. It is interesting that when $C_0 = 0.5M$, the influence of the type of anion on γ is negligible, as shown in Fig. 3. When the anion changes from phosphate to chloride, P_i increases slightly from 93 to 94.5 MPa, close to the tolerance of the testing system. The effective interfacial tension varies from 14 to 14.2 mJ/m² by only 1.5%.

As the ion concentration increases, the difference in ion transport pressures of different electrolytes becomes evident

(Fig. 2). In the sodium phosphate based system, the increase in ion concentration does not considerably affect P_i . In all the other three systems, P_i largely increases. In the sodium sulfate based system, the ion transport pressure increases by 4 MPa; correspondingly, the effective interfacial tension varies by 0.6 mJ/m². In the sodium acetate based system, the ion transport pressure increases by 8 MPa, which implies that the effective interfacial tension rises by 1.2 mJ/m². The largest increase in P_i occurs in the sodium chloride based system, which is 15 MPa. The corresponding variation in effective interfacial tension is 2.2 mJ/m². Clearly, there must be an abrupt change in configuration of confined anions when the cation concentration increases from 0.5M to 2M. When the ion concentration is relatively low, since the solid surface tends to adsorb cations, the anions would be repelled to the central part of a nanopore. Note that the cation ion diffusion and adsorption process can be fundamentally different from that at a large solid surface. The cations cannot be fully solvated since the characteristic van der Waals size of a fully solvated structure is comparable with the effective nanopore diameter. Thus, high-energy configurations that are “stretched” along the axial direction can be dominant, and the ion transport rate can be either increased or decreased, depending on the energy barrier offered by the solid atoms. As the anions move toward the interior, they are somewhat shielded by the cations and water molecules. As a result, when their concentration and ion charges vary, little variation in ion transport pressure, which reflects the system free energy variation rate, would take place.

When the ion concentration is relatively high, the inner space in the nanopore becomes insufficient for all the anions. In the ZSM-5 sample, the effective nanopore size is around 0.6 nm. If the thickness of the liquid molecular layer immediate adjacent to the solid atoms is 0.25 nm, the cross-sectional length scale of the inner space is only 1 Å. If the number of anions is increased, a portion of them would direct contact the solid atoms, and their influence on the solid-liquid interfacial tension, i.e., the ion transport pressure, would be much more pronounced (Fig. 3). Sodium phosphate is of the lowest anion concentration. Even when the cation concentration is 2M, most of the confined anions, whose concentration (0.67M) is only slightly higher than 0.5M, can still be separated from the solid atoms. Hence, the ion transport pressure is similar with that of the low ion concentration system. In the sodium sulfate solution, the anion concentration is 1M. As a certain portion of anions are in direct contact with the solid phase, they increase the system free energy. When the anion species is changed to acetate, the anion charge is decreased to 1 but the concentration is increased to 2M. The system free energy increases more evidently.

Figure 3 also indicates that the anion size is another important factor that affects the ion transport pressure. While the cation ion concentrations and the anion concentrations of the sodium chloride solution are the same with that of the sodium acetate solution, the value of P_i of the former is

higher. A major difference between the two systems is the anion size. Since chlorine anions are smaller than acetate anions, it is easier for the former to diffuse away from the central part of a nanopore and approach the solid atoms. Consequently, more anions are involved in the high-potential configurations, leading to the increase in system free energy.

In summary, in an experimental study on transport of pressurized electrolyte solutions in a ZSM-5 zeolite, it is noticed that when the anion concentration is relatively low, its influence on ion transport pressure is negligible; when the anion concentration is relatively high, its effect becomes significant. The ion size also has a pronounced influence on the system free energy. These phenomena can be attributed to the confined ion structures in nanopores.

This study was supported by The National Science Foundation and The Sandia National Laboratory under Grant No. CMS-0623973.

- ¹H. Suzuki and S. Takeuchi, *Anal. Bioanal. Chem.* **391**, 2695 (2008).
- ²F. Tadini-Bunoninsegni, G. Bartolomei, M. R. Moncelli, and K. Fendler, *Arch. Biochem. Biophys.* **476**, 75 (2008).
- ³P. Heitjans, E. Tobschall, and M. Wilkening, *Eur. Phys. J. A* **161**, 97 (2008).
- ⁴M. Chen, Y. F. Chen, W. Zhong, and J. K. Yang, *Sci. China, Ser. E: Technol. Sci.* **51**, 921 (2008).
- ⁵F. Dehez, M. Tarek, and C. Chipot, *J. Phys. Chem. B* **111**, 10633 (2007).
- ⁶P. R. Haddad and P. E. Jackson, *Ion Chromatography* (Elsevier, New York, NY, 1990).
- ⁷H. Y. Erbil, *Surface Chemistry of Solid and Liquid Interfaces* (Wiley-Blackwell, Boston, MA, 2006).
- ⁸H. Rubin, *Environmental Fluid Mechanics* (CRC, Boca Raton, FL, 2001).
- ⁹H. J. Butt, K. Graf, and M. Kappl, *Physics and Chemistry of Interfaces*, (Wiley, New York, NY, 2006).
- ¹⁰A. V. Delgado, *Interfacial Electrokinetics and Electrophoresis* (CRC, Boca Raton, FL, 2001).
- ¹¹J. Yang, F. Z. Lu, L. W. Kostiuik, and D. Y. Kwok, *J. Micromech. Microeng.* **13**, 963 (2003).
- ¹²F. H. J. van der Heyden, D. Stein, and C. Dekker, *Phys. Rev. Lett.* **95**, 116104 (2005).
- ¹³E. E. Polymeropoulos and J. Brickmann, *Annu. Rev. Biophys. Biophys. Chem.* **14**, 315 (1985).
- ¹⁴Y. Qiao, V. K. Punyamurtula, A. Han, and H. Lim, *J. Power Sources* **183**, 403 (2008).
- ¹⁵Y. Qiao, A. Han, and V. K. Punyamurtula, *J. Phys. D: Appl. Phys.* **41**, 085505 (2008).
- ¹⁶Y. Qiao, V. K. Punyamurtula, and A. Han, *Appl. Phys. Lett.* **91**, 153102 (2007).
- ¹⁷A. Han and Y. Qiao, *J. Am. Chem. Soc.* **128**, 10348 (2006).
- ¹⁸Y. Qiao, G. Cao, and X. Chen, *J. Am. Chem. Soc.* **129**, 2355 (2007).
- ¹⁹W. Dyrka, A. T. Augousti, and M. Kotulska, *J. Comput. Chem.* **29**, 1876 (2008).
- ²⁰I. Vlasiouk, S. Smirnov, and Z. Siwy, *Nano Lett.* **8**, 1978 (2008).
- ²¹J. O. Bockris and S. U. M. Khan, *Surface Electrochemistry* (Springer, New York, NY, 1993).
- ²²E. M. McCash, *Surface Chemistry* (Oxford University Press, London, UK, 2001).
- ²³A. Tanimura, A. Kovalenko, and F. Hirata, *Langmuir* **23**, 1507 (2007).
- ²⁴L. Zeng, G. H. Zuo, X. J. Gong, H. J. Lu, C. L. Wang, K. F. Wu, and R. Z. Wan, *Chin. Phys. Lett.* **25**, 1486 (2008).
- ²⁵A. Han, X. Chen, and Y. Qiao, *Langmuir* **24**, 7044 (2008).
- ²⁶A. Han and Y. Qiao, *Appl. Phys. Lett.* **91**, 173123 (2007).
- ²⁷L. Liu, Y. Qiao, and X. Chen, *Appl. Phys. Lett.* **92**, 101927 (2008).